Int. J. Electrochem. Sci., 14 **(2019)** 7947 – 7960, doi: 10.20964/2019.08.08

International Journal of
ELECTROCHEMICAL
SCIENCE
www.electrochemsci.org

Study on Thermal Stability and Corrosion Inhibition Effect of [Ni(s-htde)]$(ClO_4)_2$ for Q235 Steel in 1.0 M HCl

Wan Gou[1, 3], Wei Wang[2], Wenrong Xie[2], Ping Zhang[2], Lan Wang[2], Jing Zhang[2], Yanan Shi, Bin Xie[3]*

[1] School of Chemistry and Chemical Engineering, Eastern Sichuan Sub-center of National Engineering Research Center for Municipal Wastewater Treatment and Reuse, Sichuan University of Arts and Science, Dazhou 635000, China
[2] Selenium ProductQuality Supervision and Inspection Center of Sichuan Province, Market Supervision and Administration of Wanyuan, Wanyuan 636350, China
[3] Material Corrosion and Protection Key Laboratory of Sichuan Province, Key Laboratories of Fine Chemicals and Surfactants in Sichuan Provincial Universities, Key Laboratories of Green Catalysis of Higher Education Institutes of Sichuan, Sichuan University of Science and Engineering, Zigong 643000, Chin
[*]E-mail: scwlxygw@126.com

Received: 6 January 2019 / *Accepted:* 18 February 2019 / *Published:* 30 June 2019

Nickel (II) complexes of 5, 7, 7, 12, 14, 14-hexamethyl-1, 4, 8, 11-tetraazacyclotetradeca4, 11-diene ([Ni(us-htde)]$(ClO_4)_2$) and 5, 5, 7, 12, 12, 14-hexamethyl-1, 4, 8, 11-tetrazacyclotetradecane ([Ni(s-htde)]$(ClO_4)_2$) are synthesized and confirmed by elemental analysis. Here, the thermal stability of the two nickel (II) complexes are investigated by TG/DSC technology. Moreover, the corrosion inhibition of [Ni(s-htde)]$(ClO_4)_2$ in 1.0 M HCl is evaluated by weight loss method and potentiodynamic polarization measurement. The study results show that the thermal decomposition process of the [Ni(us-htde)] $(ClO_4)_2$ and [Ni(s-htde)]$(ClO_4)_2$ heated in N_2 and air atmospheres all proceeded in three steps, which is not affected by N_2 and air atmospheres. The thermal stability of the [Ni(s-htde)]$(ClO_4)_2$ is better than [Ni(us-htde)]$(ClO_4)_2$, which can be stable at the temperature below 283 °C and 270 °C in N_2 and air atmospheres. Meanwhile, the study results show that [Ni(s-htde)]$(ClO_4)_2$ can act as an effective mixed-type corrosion inhibitor, and it adsorption on Q235 steel surface can be described by Langmuir isotherm, which belongs to physic- and chemisorption.

Keywords: Macrocycle; Nickel complexes; Thermal stability; Decomposition; Atmospheres; Inhibitor.

1. INTRODUCTION

Macrocycles are often described as a molecule containing at least one large ring composed of 12 or more atoms [1]. In the past, most of the known synthetic macrocycles had been prepared,

characterized and reported [2-6]. Most commonly they are quadri dentates containing nitrogen donor atoms, although compounds containing sulfur and oxygen donor atoms and are also known [5, 6, 7-9].

It is well known that macrocyclic complexes have been of great interest due to their importance as an essential metalloenzyme active site. Typically the 14-membered tetraamine macrocycle cyclam (1, 4, 8, 11-tetraazacyclotetradeca and 1, 4, 8, 11-tetraazacyclotetradecane) are well recognized as an example among the macrocyclic polyamines in coordination chemistry [10-13]. Moreover, as an important research aspect of macrocyclic ligands and their complexes, the thermal stability can affect the application field, service life and storage time of these compounds [14-17]. Therefore, it is of great significance to study the thermal stability and decomposition mechanism of macrocyclic complexes.

As the classical macrocycles, the ligands and complexes of unsaturated macrocycle (us-htde, showing in figure 1) diperchlorate and saturated macrocycle (s-htde, showing in figure 1) as corrosion inhibitor and catalyst were reported in our previous works [18-22]. As a further extension study, the nickel (II) complexes of 5, 7, 7, 12, 14, 14-hexamethyl-1, 4, 8, 11-tetraazacyclotetradeca4, 11-diene ($[Ni(us\text{-}htde)](ClO_4)_2$) and 5, 5, 7, 12, 12, 14-hexamethyl-1, 4, 8, 11- tetrazacyclotetradecane ($[Ni(s\text{-}htde)](ClO_4)_2$) are synthesized, and the thermal stability of the two complexes is presented. Moreover, the corrosion inhibition of $[Ni(s\text{-}htde)](ClO_4)_2$ in 1.0 M HCl also evaluating by weight loss and potentiodynamic polarization measurements are presented.

2. MATERIALS AND METHODS

2.1 Materials

The methanol (CH_3OH), acetone (CH_3COCH_3), ethylenediamine ($NH_2CH_2CH_2NH_2$), nickel (II) acetate tetrahydrate ($Ni(CH_3COO)_2{\cdot}4H_2O$), diethyl ether ($CH_3CH_2OCH_2CH_3$), hydrochloric acid (HCl, 37%), sodium borohydride and sodium hydroxide were purchased from Kelong Chemical Reagent Co. Ltd. (China). Meanwhile, the perchloric acid ($HClO_4$, 72%) and sodium perchlorate ($NaClO_4$) were purchased from Tianjin Xinyuan chemical Co. Ltd (China). Q235 steel samples were purchased from Chengdu Kuntai technology co., LTD. All these analytically pure chemicals are not further purified before used.

2.2 Synthesis of macrocyclic ligands and their nickel (II) complexes

In order to synthesize the nickel (II) complexes of 5, 7, 7, 12, 14, 14-hexamethyl-1, 4, 8, 11-tetraazacyclotetradeca4, 11-diene ($[Ni(us\text{-}htde)](ClO_4)_2$) and 5, 5, 7, 12, 12, 14-hexamethyl-1, 4, 8, 11-tetrazacyclotetradecane ($[Ni(s\text{-}htde)](ClO_4)_2$), the macrocyclic ligands of 5, 7, 7, 12, 14, 14-hexamethyl-1, 4, 8, 11-tetraazacyclotetradeca-4, 11-diene diperchlorate ($us\text{-}htde{\cdot}2HClO_4$) and 5, 5, 7, 12, 12, 14-hexamethyl-1, 4, 8, 11-tetrazacyclotetradecane ($s\text{-}htde{\cdot}2H_2O$) as the precursor compounds are synthesized by the reaction of acetone, ethylenediamine, perchloric acid and sodium borohydride describing in reference [21, 22, 23].

After the macrocyclic ligands prepared, the two groups of nickel (II) acetate tetrahydrate ($Ni(CH_3COO)_2 \cdot 4H_2O$, 0.2 mol) will be dissolved in 500 ml methanol in a 1 L beaker respectively, then 91 g and 61g us-htde·$2HClO_4$ and s-htde·$2H_2O$ are added respectively for preparing the nickel (II) complexes of $[Ni(us\text{-}htde)](ClO_4)_2$ and $[Ni(s\text{-}htde)](ClO_4)_2$. A slight excess of nickel (II) acetate tetrahydrate is needed to ensure the complete reaction for the macrocyclic ligands. When nickel (II) acetate tetrahydrate and the macrocyclic ligands are fully mixed in methanol, which will be stirred for 6 hours at 40 °C and cooled rapidly in a refrigerator, and the yellow crystals of the racemic isomer are removed by filtration. The crystals are washed with methanol and diethyl ether and dried in a vacuum oven at 80 °C for 2 hours. Here, the target nickel (II) complexes of $[Ni(us\text{-}htde)](ClO_4)_2$ and $[Ni(s\text{-}htde)](ClO_4)_2$ are shown in figure 1.

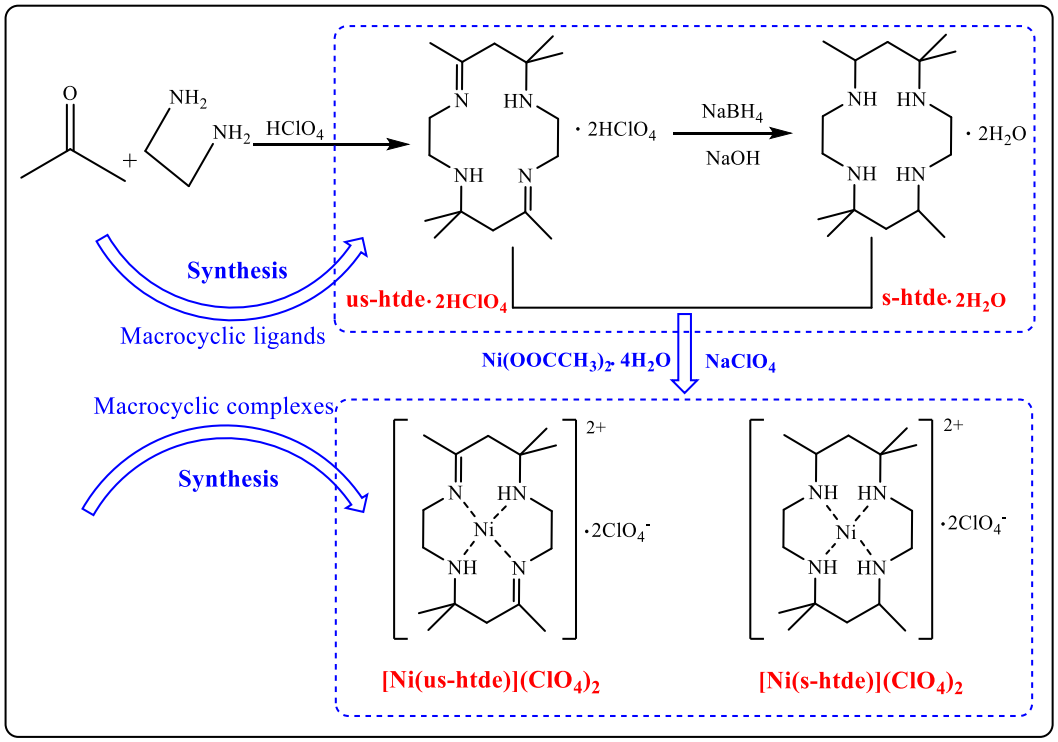

Figure 1. Reaction routs and structure of the target nickel (II) complexes of $[Ni(us\text{-}htde)](ClO_4)_2$ and $[Ni(s\text{-}htde)](ClO_4)_2$.

Table 1. The elemental analysis results of macrocyclic ligands and their nickel (II) complexes.

Compounds	Molecular formula	Found			Anal. Calcd.			Literature [23]		
		C /%	H /%	N /%	C /%	H /%	N /%	C /%	H /%	N /%
us-htde·$2HClO_4$	$C_{16}H_{34}Cl_2O_8N_4$	39.88	7.21	11.66	39.92	7.07	11.64	40.06	7.10	11.63
s-htde·$2H_2O$	$C_{16}H_{40}O_2N_4$	60.44	11.89	17.63	60.00	12.50	17.50	60.11	12.58	17.27
$[Ni(us\text{-}htde)](ClO_4)_2$	$C_{16}H_{32}Cl_2O_8N_4Ni$	35.88	5.94	10.44	35.71	5.95	10.41	35.80	6.01	10.51
$[Ni(s\text{-}htde)](ClO_4)_2$	$C_{16}H_{36}Cl_2O_8N_4Ni$	35.58	6.31	10.38	35.45	6.69	10.37	35.61	6.49	10.40

In addition, in order to confirm the two macrocyclic ligands and their nickel (II) complexes, the elemental analysis as the most direct method is used to analyze the chemical composition of us-

htde·2HClO$_4$, s-htde·2H$_2$O, [Ni(us-htde)](ClO$_4$)$_2$ and [Ni(s-htde)](ClO$_4$)$_2$, and results are listed in table 1. Comparing the value of calculated (Anal. Calcd.), literature (Literature [23]) and observed data (Anal. Found), which is in good agreement and fit well with the structure of macrocyclic ligands and their nickel (II) complexes showing in figure 1.

2.3 Thermal stability

The thermal stability evaluation by TG, DTG and DSC are performed with the Netzsch STA 409 PC/PG thermal analyzer in temperature range from 25 ℃ to 850 ℃ at different heating rates of 5, 10 and 20 ℃ min^{-1}. The measurement on thermal analysis were taken using sample masses of 8.0-11.0 mg in open alumina sample holders under both dynamic dry air and N_2 atmospheres with a discharge rate of 100 mL min^{-1} at atmosphere pressure.

2.4 Corrosion inhibition evaluation

Weight loss measurement to evaluate corrosion inhibition was described in presented works [24-25]. Here, the corrosion rate (v) and inhibition efficiency (IE_{WL}, %) of Q235 in 1.0 M HCl with different concentrations of [Ni(s-htde)](ClO$_4$)$_2$ were calculated by equation (1) and (2). Where m_0 and m_i are the mass of the test samples before and after corrosion, S = 28.0 cm^2, t is the immersion time, v_i and v_0 are corrosion rate of Q235 sample in 1.0 M HCl with different concentrations of [Ni(s-htde)](ClO$_4$)$_2$.

$$v_i = \frac{m_0 - m_i}{St} \quad (1)$$

$$IE_{WL}\ (\%) = \frac{v_0 - v_i}{v_0} \times 100\% \quad (2)$$

Potentiodynamic polarization measurement to evaluate corrosion inhibition was conducted by conventional three-electrode system carrying out by CHI 760E electrochemical workstation using the Pt electrode and SCE (saturated calomel reference electrode) as the counter and reference electrode, the potential sweep rate was 0.5 mV s^{-1}. The inhibition efficiency (IE_{Tafel}, %) obtained by this method can be calculated by equation (3) [22, 24, 25]. Where i_i and i_0 are the corrosion current density values of Q235 electrode corrosion in 1.0 M HCl with different concentrations of [Ni(s-htde)](ClO$_4$)$_2$.

$$IE_{Tafel}\ (\%) = \frac{i_0 - i_i}{i_0} \times 100\% \quad (3)$$

3. RESULTS AND DISCUSSION

3.1 Thermal stability of [Ni(s-htde)](ClO$_4$)$_2$

Thermal stability of [Ni(s-htde)](ClO$_4$)$_2$ is studied by TG/DSC analysis. Here, the TG curves, DTG curves and DSC curves obtained under the N_2 atmosphere at the heating rates of 5, 10 and 20 °C min^{-1} show in figure 2, 3 and 4.

3.1.1 TG curves of [Ni(s-htde)](ClO_4)$_2$

From TG and their magnification curves showing in figure 2 (a) and (b), which present that the thermal decomposition process of [Ni(s-htde)](ClO_4)$_2$ under N_2 atmosphere at 5, 10 and 20 °C min^{-1} all proceeded in three steps. This is similar to the previously reported on nickel (II) complex 5, 7, 7, 12, 14, 14-hexamethyl-1, 4, 8, 11-tetraazacyclotetradeca4, 11-diene ([Ni(htde)](ClO_4)$_2$) decomposition [22]. At the heating rate of 5 °C min^{-1}, the first step attribute to the thermal oxidation degradation of macrocyclic ligand (s-htde) by perchlorate (ClO_4^-) in the temperature range from 283 °C to 338 °C. The second step in the temperature range of 338 - 365 °C is corresponding to the decomposition of one H_2O molecule. And the third step of mass loss in the temperature range of 365 - 790 °C, it is caused by the loss of diethylamine ligands obtained by macrocyclic ligand (s-htde) decomposition at high temperatures (> 365 °C).

Under TG analysis conditions, although the heating rate is different, all the TG curves have similar trends. Moreover, it can be found that [Ni(s-htde)](ClO_4)$_2$ demonstrates mass loss 31.12%, 3.22% and 25.62% in the first, second and third step at the heating rate of 5 °C min^{-1} respectively, this results is due to the successive loss of two 2-methylpentane, H_2O molecule and two diethylamine ligands. From the TG magnification curves (figure 2 (b)), which exhibit that the mass loss of the complex of [Ni(s-htde)](ClO_4)$_2$ do not destruct at the temperature below 283 °C, which further suggests that [Ni(s-htde)](ClO_4)$_2$ can be stable at the temperature below 283 °C under the N_2 atmosphere. One interesting finding is that when the heating temperature increased to 366.3 °C with different heating rates, all the TG curves converge at the mass loss of 34.41%. Furthermore, when the temperature increases to 800 °C, all the TG curves tends to be stable as the temperature further increase, which indicates that the decomposition of residue will not be further decomposed after the temperature exceeds 800 °C. And with the heating temperature increase from room temperature to 850 °C, that the mass loss is 59.96%.

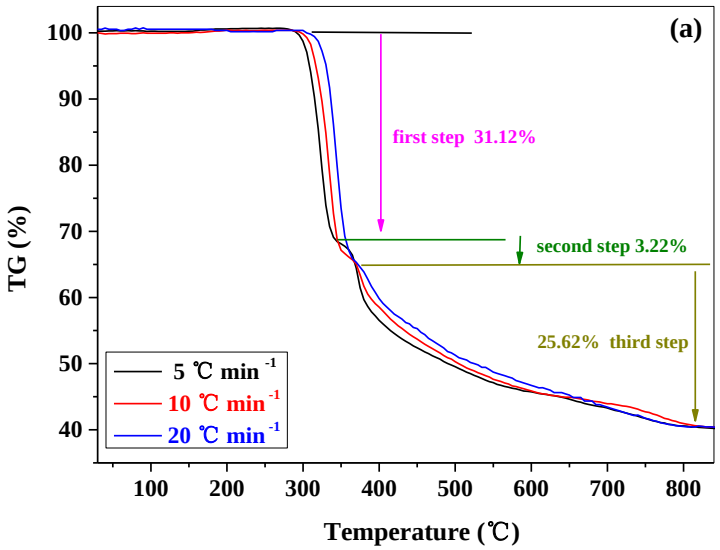

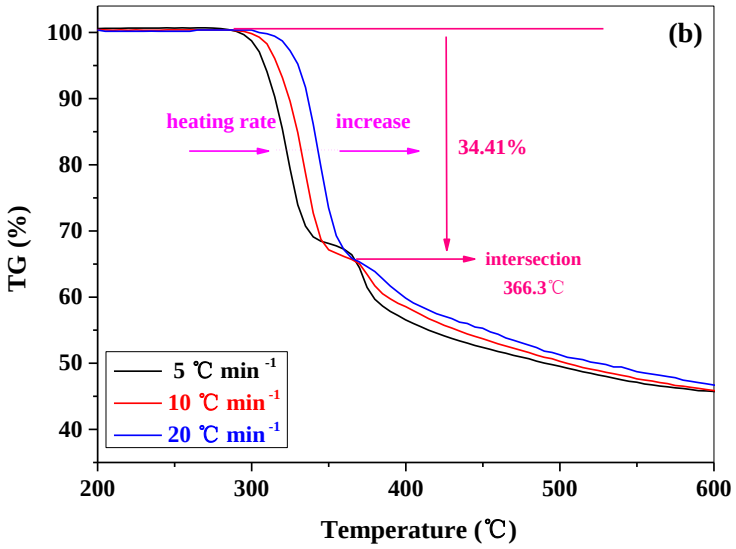

Figure 2. TG (a) and their magnification curves (b) for [Ni(s-htde)]$(ClO_4)_2$ heated under N_2 atmosphere at the heating rates of 5, 10 and 20 °C min^{-1}.

3.1.2 DTG curves of [Ni(s-htde)]$(ClO_4)_2$

The DTG and their magnification curves of [Ni(s-htde)]$(ClO_4)_2$ heated under N_2 atmosphere at the heating rates of 5, 10 and 20 °C min^{-1} present in figure 3 (a) and (b), which is the derivative of thermogravimetric analysis (TG). According to the DTG curves, it can be seen that with the heated temperature increase, there are two obvious peaks presenting in the each DTG curves. The heated temperature ($T_{p\text{-}DTG1}$, $T_{p\text{-}DTG2}$) of the peaks values of each curve are listed in table 2. The two peaks correspond to the first and second mass loss processes of [Ni(s-htde)] $(ClO_4)_2$. Obviously, the $T_{p\text{-}DTG1}$ and $T_{p\text{-}DTG2}$ increases with the increase of the heating rates.

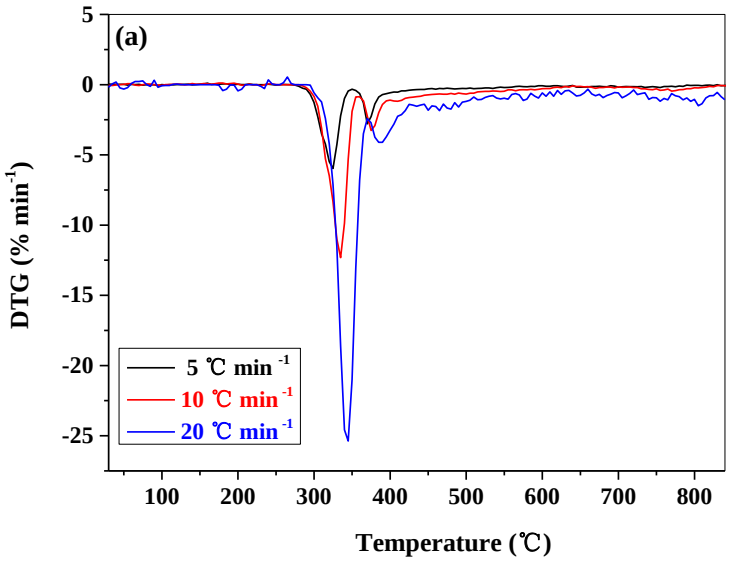

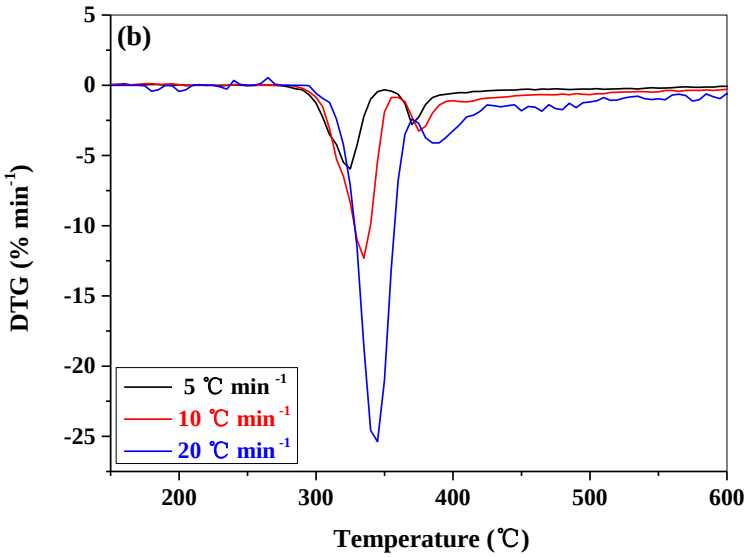

Figure 3. DTG (a) and their magnification curves (b) for [Ni(s-htde)]$(ClO_4)_2$ heated under N_2 atmosphere at the heating rates of 5, 10 and 20 °C min^{-1}.

Table 2. The heated temperature of the peaks values of each DTG curves for [Ni(s-htde)]$(ClO_4)_2$ heated under N_2 atmosphere at the heating rates of 5, 10 and 20 °C min^{-1}.

v (°C min^{-1})	$T_{p\text{-}DTG1}$ (°C)	$T_{p\text{-}DTG2}$ (°C)
5	323.5	366.5
10	334.7	374.9
20	343.1	381.5

3.1.3 DSC curves of [Ni(s-htde)]$(ClO_4)_2$

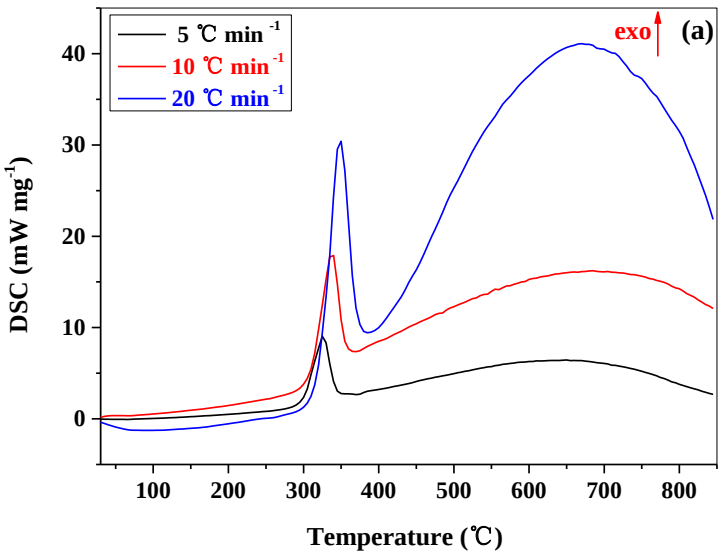

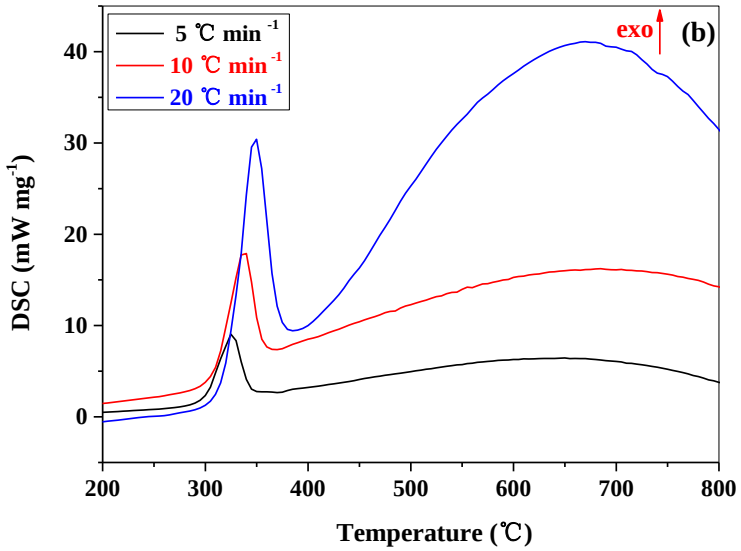

Figure 4. DSC (a) and their magnification curves (b) for [Ni(s-htde)]$(ClO_4)_2$ heated under N_2 atmosphere at the heating rates of 5, 10 and 20 °C min^{-1}.

Based on DSC and their magnification curves presenting in figure 4 (a) and (b), it hard to find any obvious endothermic peaks during heating of [Ni(s-htde)]$(ClO_4)_2$ in N_2 atmosphere at different heating rates, but instead there are two strong exothermic peaks on each DSC curves at the heating rates of 5, 10 and 20 °C min^{-1}. So it is conferred that the process of heating [Ni(s-htde)]$(ClO_4)_2$ is a self-oxidation and destruction process between perchlorate (ClO_4^-) and macrocyclic ligand of s-htde, which belongs to a strong exothermic process. In the heating process, the heat released will cover up with the heat absorbed, so only exothermic peaks will present in the curves instead of endothermic peaks. The first sharp peaks and second wide peaks are listed in table 3 ($T_{p\text{-}DSC1}$ and $T_{p\text{-}DSC2}$), and appeared in DSC curves at the temperature range of 300 °C to 350 °C and 640 °C to 800 °C, respectively.

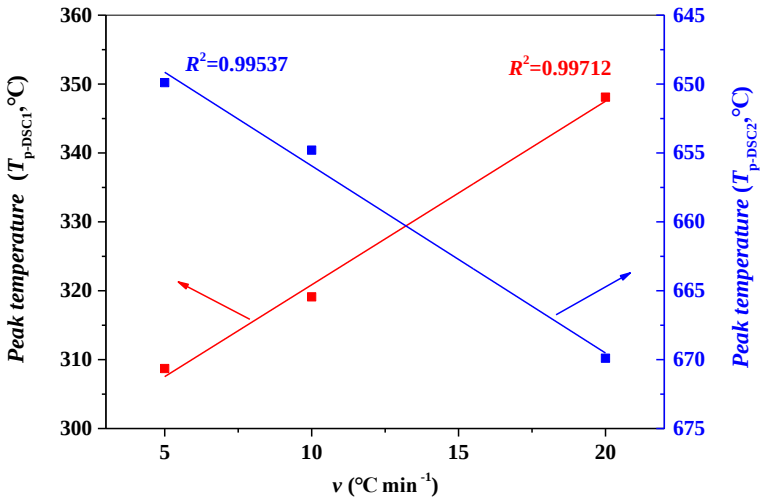

Figure 5. Fitting result between exothermic peak temperature ($T_{p\text{-}DSC1}$ and $T_{p\text{-}DSC2}$, °C) and heating rates for [Ni(s-htde)]$(ClO_4)_2$ heated under N_2 atmosphere.

Table 3. The exothermic peaks for [Ni(s-htde)]$(ClO_4)_2$ heated under N_2 atmosphere at the heating rates of 5, 10 and 20 °C min^{-1}.

v (°C min^{-1})	$T_{p\text{-}DSC1}$ (°C)	$T_{p\text{-}DSC2}$ (°C)
5	308.7	649.9
10	319.1	654.8
20	348.1	669.9

In addition, based on the data listing in table 3, the fitting result between the temperature of exothermic peaks and heating rates for [Ni(s-htde)]$(ClO_4)_2$ heated in N_2 atmosphere is shown in figure 5. It can be seen from the figure that the temperature of exothermic peaks ($T_{p\text{-}DSC1}$ and $T_{p\text{-}DSC2}$, °C) increases with the increase of the heating rates (v, °C min^{-1}), and there are the strong linear relationship (R^2 = 0.99502) between the heating rates and the peaks temperature, which can be expressed by $T_{p\text{-}DSC1}$ (°C) = 294.2 + 2.67 v and $T_{p\text{-}DSC2}$ (°C) = 642.4 + 1.36 v.

3.2 The effect of atmospheres on thermal stability of [Ni(s-htde)]$(ClO_4)_2$

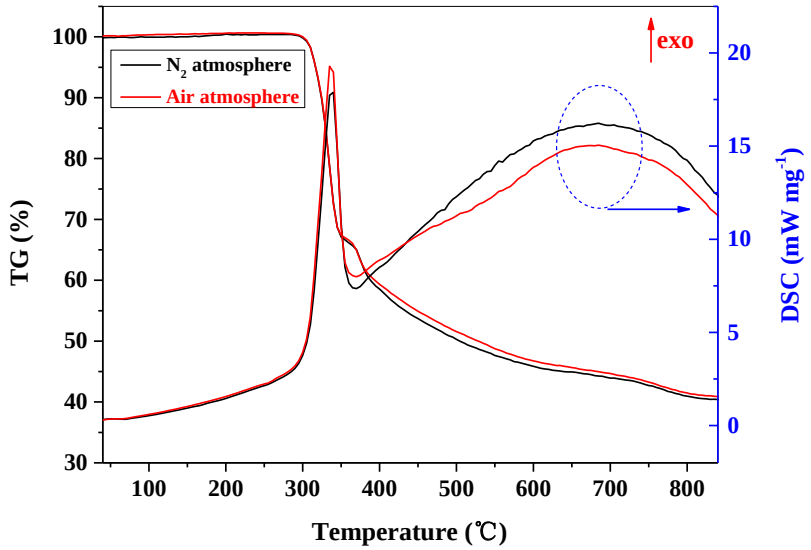

Figure 6. TG/DSC curves for [Ni(s-htde)]$(ClO_4)_2$ heated in air and N_2 atmospheres at 10 °C min^{-1}.

Moreover, the thermal stability of [Ni(s-htde)]$(ClO_4)_2$ in different atmospheres (air and N_2) is studied by TG/DSC curves for heating [Ni(s-htde)]$(ClO_4)_2$ at 10 °C min^{-1} showing in figure 6. Comparison TG curves and DSC curves obtained under the N_2 and air atmospheres, it is clearly that the TG curve is almost the same variation tendency for [Ni(s-htde)]$(ClO_4)_2$ heated in N_2 and air atmospheres. This indicates that the thermal decomposition mechanism of [Ni(s-htde)]$(ClO_4)_2$ heated will not change either in N_2 atmosphere or in air atmosphere, in other words, the thermal decomposition mechanism of [Ni(s-htde)]$(ClO_4)_2$ heated is not affected by N_2 and air atmospheres.

Under the temperature more than 300 °C, the DSC curve does not overlap, which may be due to the baseline drift during the test.

3.3 Comparison the thermal stability of [Ni(s-htde)](ClO4)2 and [Ni(us-htde)](ClO4)2

In order to further explore the thermal stability and thermal decomposition mechanism of the fully saturated macrocyclic complex of [Ni(s-htde)](ClO4)2, the unsaturated macrocyclic complex of [Ni(us-htde)](ClO4)2 as the comparison and precursor compound is heated in N2 atmosphere at 5 °C min^{-1} to evaluate the thermal stability by TG and DSC analysis, and the TG/DSC curves of [Ni(s-htde)](ClO4)2 and [Ni(us-htde)](ClO4)2 are shown in figure 7.

It can be seen from the figure that the variation trend of the TG curves and DSC curves of [Ni(s-htde)](ClO4)2 and [Ni(us-htde)](ClO4)2 are similar but not identical. There are all three steps mass loss and finally tend to be stable in TG curves, but the different decomposition temperatures and different thermal effects for the two complexes. Moreover, the [Ni(us-htde)](ClO4)2 TG curve demonstrates that the mass loss are 29.63%, 17.25% and 8.95% in the first to third step. According to TG curve, the thermal decomposition temperature of saturated macrocyclic complex [Ni(s-htde)](ClO4)2 is higher than that of unsaturated macrocyclic complex [Ni(us-htde)](ClO4)2, indicating that the thermal stability of the [Ni(s-htde)](ClO4)2 is better than [Ni(us-htde)](ClO4)2. This due to the greater coordination between N atoms and nickel (II) in the [Ni(us-htde)](ClO4)2.

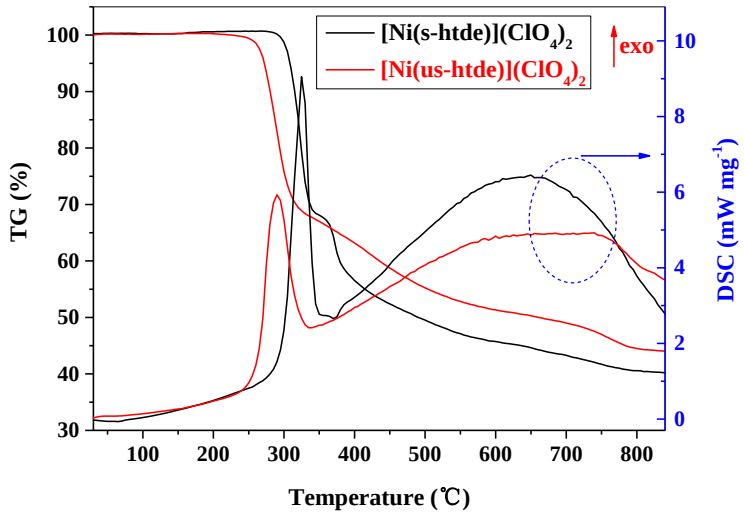

Figure 7. TG/DSC curves of [Ni(s-htde)](ClO4)2 and [Ni(us-htde)](ClO4)2 heated in N2 atmosphere at 5 °C min^{-1}.

3.4 Corrosion inhibition

3.4.1 Weight loss measurement

Weight loss measurement results for Q235 steel corrosion in 1.0 M HCl with various concentrations of [Ni(s-htde)](ClO4)2 at 30 °C are listed in table 4. It can be found that inhibition

efficiency (IE_{WL}, %) increased with [Ni(s-htde)]$(ClO_4)_2$ concentration (C, mg L^{-1}) increasing. When the concentration of corrosion inhibitor increases to 100 mg L^{-1}, the corrosion inhibition efficiency (IE_{WL}, %) reaches 86.63%. As the concentration continues to increase, the corrosion inhibition efficiency tends to be stable. The similar tendency were reported by S-4-methylbenzyl-O,O'-di(phenyl)dithiophosphate [26], S-4-methylbenzyl-O,O'-di(4-bromophenyl)dithiophosphate[26]and 2-(*p*-bromobenzylthio)-1*H*-benzimidazole [27] as corrosion inhibitor in HCl solution. This increase tendency is caused by the balance of the adsorption and desorption of [Ni(s-htde)]$(ClO_4)_2$ on Q235 steel surface.

Based on the molecular structure of [Ni(s-htde)]$(ClO_4)_2$, that the corrosion inhibition performance of [Ni(s-htde)]$(ClO_4)_2$ is probably affected by two factors [22]. On the one hand, the perchlorate (ClO_4^-) as anion present in the molecular structure of [Ni(s-htde)]$(ClO_4)_2$, which has the oxidation property that can lead to the formation of oxide film on the Q235 steel surface and thus play a role in corrosion inhibition. On the other hand, under acidic conditions (1.0 M HCl), due to the dissociation of saturated macrocyclic ligand (s-htde) from [Ni(s-htde)]$(ClO_4)_2$. Because the lone pair electrons of N atoms presenting in s-htde can interact with iron atoms on the surface of Q235 steel thus acting as a corrosion inhibitor. Therefore, the corrosion inhibition is caused by both the oxidation of perchlorate and the adsorption of N atoms in saturated macrocyclic ligand of s-htde.

Table 4. Weight loss measurement results for Q235 steel in 1.0 M HCl with various concentrations of [Ni(s-htde)]$(ClO_4)_2$ at 30 ℃.

Concentration (C, mg L^{-1})	20	60	80	100	150	200
IE_{WL} (%)	65.32	76.74	79.36	86.63	87.02	87.31

3.4.2 Potentiodynamic polarization measurement

Polarization curves obtained by potentiodynamic polarization measurement for Q235 steel in 1.0 M HCl with different concentrations of [Ni(s-htde)]$(ClO_4)_2$ at 30°C is shown in figure 8. The inhibition efficiency (IE_{Tafel}, %) obtained by this method based on equation (3) are listed in table 5. Moreover, the other electrochemical parameters contained i_i (μA cm^{-2}), E vs SCE (V), β_c and β_a (mV dec^{-1}) are also presented in table 5.

From the figure and table, it can be found that both the anodic and cathodic curves shift to lower current densities for Q235 steel in 1.0 M HCl with [Ni(s-htde)]$(ClO_4)_2$ concentration increased. The decrease of i_i is due to [Ni(s-htde)]$(ClO_4)_2$ adsorbing on Q235 steel surface to form a protective film. As [Ni(s-htde)]$(ClO_4)_2$ concentration increased from 20 mg L^{-1} to 100 mg L^{-1}, the IE_{Tafel} increased from 58.8% to 84.4%. Comparison with some other reported compounds such as ketoconazole [28], 2-(quinolin-2-yl)quinazolin-4(3H)-one [29] and riboflavin [30] as corrosion inhibitor for Q235 steel in 1.0 M HCl, which showed that the inhibition efficiency are 88.8% (303 K, 80mg L^{-1}), 87.0 % (25 ℃, 0.111 mM) and 83.9% (30 ℃, 0.0012 M), respectively, for Q235 steel corrosion in 1 M HCl solution according to potentiodynamic polarization results. It is found that [Ni(us-htde)]$(ClO_4)_2$ can act as an effective inhibitor. Meanwhile, the corrosion inhibition effect of

[Ni(s-htde)]$(ClO_4)_2$ is better than that of the nickel (II) complex 5, 7, 7, 12, 14, 14-hexamethyl-1, 4, 8, 11-tetraazacyclotetradeca4, 11-diene ([Ni(htde)]$(ClO_4)_2$) [22], this is mainly because the rigidity of saturated macyclic molecules ([Ni(s-htde)]$(ClO_4)_2$) is weaker than that of unsaturated macyclic molecules ([Ni(htde)]$(ClO_4)_2$), and the weak rigidity is conducive to corrosion inhibitor adsorption on steel surface. Additionally, the *E* vs SCE for Q235 steel in 1.0 M HCl with various concentration of [Ni(s-htde)]$(ClO_4)_2$ at 30°C change slightly (＜10 mV), which shows that [Ni(s-htde)]$(ClO_4)_2$ is a mixed-type inhibitor [21, 22].

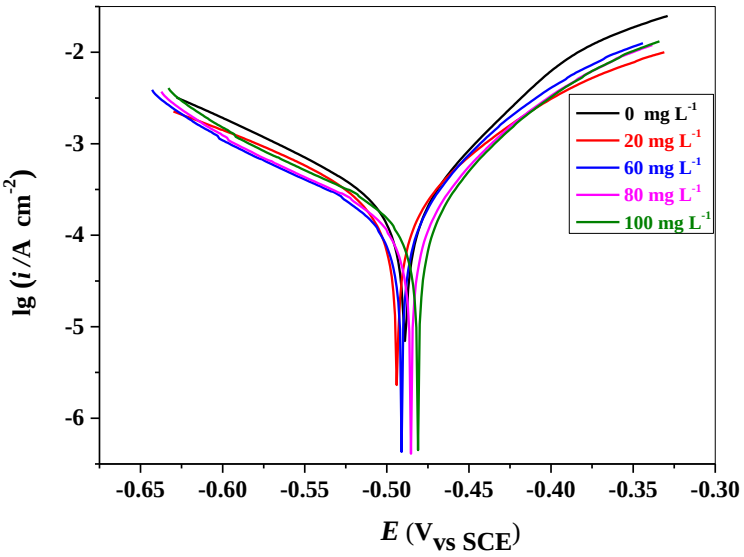

Figure 5. Polarization curves for Q235 steel in 1.0 M HCl with different concentrations of [Ni(us-htde)]$(ClO_4)_2$ at 30 °C by potentiodynamic polarization measurement.

Table 5. Electrochemical parameters for Q235 steel in 1.0 M HCl with different concentrations of [Ni(us-htde)]$(ClO_4)_2$ at 30°C.

c (mg L^{-1})	*E* (V)	β_a (mV dec^{-1}) × 10^2	β_c (mV dec^{-1}) × 10^2	i_i (μA cm^{-2}) × 10^3	IE_{Tafel} (%)
Blank solution	-0.487	1.35	1.18	1.88	-
20	-0.492	1.22	1.11	7.74	58.8
60	-0.490	1.13	1.05	6.51	65.3
80	-0.482	1.07	0.968	3.80	79.8
100	-0.478	0.994	0.899	2.92	84.4

3.5 Adsorption isotherm

Based on weight loss measurement results listing in table 4, Langmuir adsorption isotherm is employed to study the adsorption of [Ni(s-htde)]$(ClO_4)_2$ on Q235 surface in 1.0 M HCl, and the fitting result reveals at figure 9. In this figure, C/θ versus C show the strong linear relationship (R^2 = 0.99926) for Q235 steel corrosion in 1.0 M HCl, and which suggests that the adsorption of [Ni(s-htde)]$(ClO_4)_2$ on Q235 surface can be described by Langmuir isotherm. The adsorption standard free energy (ΔG)

calculating by $\Delta G = -RT\ln(55.5K)$ is -37.48 kJ mol^{-1} ($\Delta G > -40.00$ kJ mol^{-1}), which shows that the adsorption of [Ni(s-htde)]$(ClO_4)_2$ on Q235 steel surface in HCl solution belongs to the mixed adsorption which involve both the physic- and chemisorption [31-33].

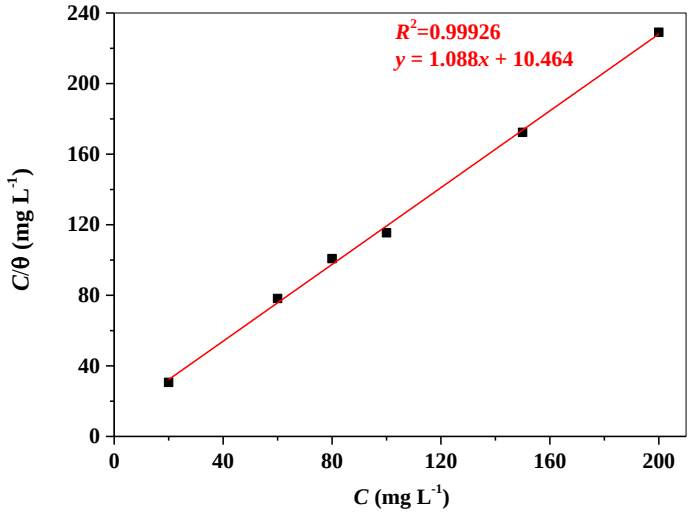

Figure 9. The fitting results of Langmuir adsorption isotherm for [Ni(s-htde)]$(ClO_4)_2$ on Q235 steel surface in 1.0 M HCl at 30 °C.

4. CONCLUSIONS

In this work, the nickel (II) complexes of 5, 7, 7, 12, 14, 14-hexamethyl-1, 4, 8, 11-tetraaza-cyclotetradeca4, 11-diene ([Ni(us-htde)]$(ClO_4)_2$) and 5, 5, 7, 12, 12, 14-hexamethyl-1, 4, 8, 11-tetraza-cyclotetradecane ([Ni(s-htde)]$(ClO_4)_2$) were successfully synthesized and confirmed by elemental analysis. Study results show that the thermal decomposition process of the [Ni(us-htde)] $(ClO_4)_2$ and [Ni(s-htde)]$(ClO_4)_2$ heated under N_2 and air atmospheres all proceeded in three steps, which is not affected by N_2 and air atmospheres. The process of [Ni(s-htde)]$(ClO_4)_2$ heating is a self-oxidation and destruction process between perchlorate (ClO_4^-) and macrocyclic ligands of s-htde and us-htde, which belongs to a strong exothermic process. The thermal stability of the [Ni(s-htde)]$(ClO_4)_2$ is better than [Ni(us-htde)]$(ClO_4)_2$, the two complexes can be stable at the temperature below 283 °C and 270 °C N_2 and air atmospheres. [Ni(s-htde)]$(ClO_4)_2$ can act as an effective mixed-type corrosion inhibitor, and that adsorption on Q235 steel surface can be described by Langmuir isotherm, which belongs to physic- and chemisorption.

ACKNOWLEDGMENTS
This project is supported by the program of Market Supervision and Administration of Wanyuan (No. 2018- 5117- 2400- 0054), the opening projects of Material Corrosion and Protection Key Laboratory of Sichuan Province (No. 2017CL02) and the Key Laboratories of Fine Chemicals and Surfactants in Sichuan Provincial Universities (Nos. 2018JXZ01, 2016JXZ03), the Key Laboratories of Green Catalysis of Higher Education Institutes of Sichuan (No. LZJ1803), the program of Science and Technology Department of Sichuan Province (Nos. 2018JY0061, 2018JY0335).

References

1. E. Marsault, M. L. Peterson, *J. Med. Chem*., 54 (2011) 1961.
2. M. Shin, H. Ju, Y. Habata, S. S. Lee, *Inorg. Chim. Acta*, 482 (2018) 749.
3. H. S. Soor, S. D. Appavoo, A. K. Yudin, *Bioorgan. Med. Chem.,* 26 (2018) 2774.
4. K. Mochizuki, T. Sugita, F. Yamada, N. Mochizuki, K. Hayano, Y. Ohgami, *Inorg. Chim. Acta*, 362 (2009) 1204.
5. E. Simon, P. L. Haridon, R. Pichon, M. L. Her, *Inorg. Chim. Acta*, 282 (1998) 173.
6. S. Brooker, *Coordin. Chem. Rev.,* 222 (2001) 33.
7. I. Bhugun, F. C. Anson, *J. Electroanal. Chem*., 430 (1997) 155.
8. J. Costamagna, G. Ferraudi, B. Matsuhiro, M. C. Vallette, J. Canales, M. Villagrán, J. Vargas, M. J. Aguirre, *Coordin. Chem. Rev.*, 1996 (2000) 125.
9. E. S. Rapaport, A. Masarwa, H. Cohen, D. Meyerstein, *Inorg. Chim. Acta*, 307 (2000) 42.
10. M. Lachkar, I. Halime, A. Bezgour, B. E. Bali, M. Dusek, K. Fejfarova, S. Siddiq, B. P. Marasini, S. Noreen, A. Khan, S. Rasheed, M. I. Choudhary, *Med. Chem. Res*., 21 (2012) 4290.
11. E. S. Rapaport, A. Masarwa, H. Cohen, D. Meyerstein, *Inorg. Chim. Acta*, 299 (2000) 41.
12. M. Shi, J. Yang, Y. Y. Liu, J. F. Ma, *Dyes Pigments*, 129 (2016) 109.
13. N. F. Curtis, *Inorg. Chim. Acta*, 317 (2001) 27.
14. H. T. Zong, L. Y. Bian, J. Y. Cheng, G. H. Cao, C. Y. Kang, M. Li, *Results Phys*., 6 (2016) 1157.
15. S. X. Wang, L. Lin, Z. C. Tan, Y. S. Li, Y. Li, *Acta Chim. Sinica,* 68 (2010) 2156.
16. V. P. Sinditskii, T. H. Hoang, A. D. Smirnova, V. Y. Egorshev, N. V. Yudin, I. A. Vatsadze, I. L. Dalinger, *Thermochim. Acta*, 667 (2018) 1.
17. M. A. Ciciliati, J. H. F. Jesus, E. T. G. Cavalheiro, *Thermochim. Acta*, 668 (2018) 33.
18. C. Huang, S. L. Cai, L. K. Zou, J. S. Feng, J. Q. Xie, B. Xie, *J. Disper. Sci. Technol*, 33 (2012) 1292.
19. S. L. Cai, W. Hu, J. Z. Li, B. Xie, L. J. He, X. L. Zhang, *Prog. React. Kinet. Mec*., 38 (2013), 240.
20. S. L. Cai , W. Hu , J. Z. Li , B. Xie , L. J. He, X. L. Zhang, *J. Disper. Sci. Technol,* 35 (2014) 93.
21. W. Gou, C. Lai, Z. Xiang, L. Yang, P. Zhang, W. K. Xie, L. Chen, G. B. Luo, X. L. Li, Z. X. Chen, *Int. J. Electrochem. Sci*., 12 (2017) 11742.
22. W. Gou, B. Xie, C. Xu, Z. Zheng, J. He, D. Huang and N. Geng, *Int. J. Electrochem. Sci.,* 14 (2019) 494.
23. B. E. Douglas, *Inorganic Syntheses*, 18 (1978) 1.
24. X. Zhang and B. Tan, *Int. J. Electrochem. Sci*., 13 (2018) 11388.
25. I. H. Ali, R. Marzouki, Y. B. Smida, A. Brahmia and M. Faouzi Zid, *Int. J. Electrochem. Sci.,* 13 (2018) 11580.
26. C. Lai, X. Guo, J. Wei, B. Xie, L. Zou, X. Li, Z. Chen, C. Wang, *Open Chem.*, 15 (2017) 263.
27. C. Lai, H. Yang, X. Guo, X. Su, L. Zhou, L. Zhang, B. Xie, *Int. J. Electrochem. Sci.*, 11 (2016) 10462.
28. Y. W. Liu, Y. Chen, X. H. Chen, Z. N. Yang, Y. Xie, Z. Zhang, *J. Alloy. Compd.*, 758 (2018)184.
29. W. W. Zhang, R. Ma, H. H. Liu, Y. Liu, S. Li, L. Niu, *J. Mol. Liq.*, 222 (2016) 671.
30. M. A.Chidiebere, E. E. Oguzie, L. Liu, Y. Li, F. H. Wang, *Mater. Chem. Phys.*, 156 (2015) 95.
31. Q. Zhao, *Int. J. Electrochem. Sci.,* 14 (2019) 2027.
32. A. Fawzy, M. Abdallah, M. Alfakeer and H. M. Ali, *Int. J. Electrochem. Sci*., 14 (2019) 2063.
33. A. E. Vázquez, F. J. R. Gómez, G. E. N. Silva, D. A. Beltrán and R. G. Olvera, *Int. J. Electrochem. Sci.,* 13 (2018) 12294.